Pharmaceutical Research, Vol. 27, No. 2, February 2010 (© 2009)
DOI: 10.1007/s11095-009-0028-7

Research Paper

PLGA Microparticles in Respirable Sizes Enhance an *In Vitro* T Cell Response to Recombinant *Mycobacterium Tuberculosis* Antigen TB10.4-Ag85B

Shuai Shi[1] and Anthony J. Hickey[1,2]

Received October 29, 2009; accepted December 3, 2009; published online December 19, 2009

Purpose. To study the use of poly (lactide-co-glycolide) (PLGA) microparticles in respirable sizes as carriers for recombinant tuberculosis (TB) antigen, TB10.4-Ag85B, with the ultimate goal of pulmonary delivery as vaccine for the prevention of TB.
Materials and Methods. Recombinant TB antigens were purified from *E. coli* by FPLC and encapsulated into PLGA microparticles by emulsion/spray-drying. Spray-drying condition was optimized by half-factorial design. Microparticles encapsulating TB antigens were assessed for their ability to deliver antigens to macrophages for subsequent presentation by employing an *in vitro* antigen presentation assay specific to an Ag85B epitope.
Results. Spray-drying condition was optimized to prepare PLGA microparticles suitable for pulmonary delivery (aerodynamic diameter of 3.3 μm). Antigen release from particles exhibited an initial burst release followed by sustained release up to 10 days. Antigens encapsulated into PLGA microparticles induced much stronger interleukin-2 secretion in a T-lymphocyte assay compared to antigen solutions for three particle formulations. Macrophages pulsed with PLGA-MDP-TB10.4-Ag85B demonstrated extended epitope presentation.
Conclusion. PLGA microparticles in respirable sizes were effective in delivering recombinant TB10.4-Ag85B in an immunologically relevant manner to macrophages. These results set the foundation for further investigation into the potential use of PLGA particles for pulmonary delivery of vaccines to prevent *Mycobacterium tuberculosis* infection.

KEY WORDS: aerosol; microparticles; *Mycobacterium tuberculosis*; spray-drying; TB10.4-Ag85B.

INTRODUCTION

Tuberculosis (TB) is the leading cause of mortality in the world (1,2). Currently, Bacillus Calmette-Guérin (BCG) is the only TB vaccine available for human use (3). However, BCG demonstrated varying levels of efficacy in distinct populations and different field trials (4,5), which can be explained partly by the waning of protective efficacy after approximately 10–15 years (6). BCG revaccination has been reported to confer no additional protection (7); hence, although effective against childhood TB (8,9), BCG has limited use against adult pulmonary disease. Therefore, there is an urgent need to develop more effective vaccine either for prophylactic use or as a booster vaccine for BCG. Among those under active investigation, subunit vaccine represents a promising vaccine candidate for its simplicity and safety (10). Although frequently administrated by parenteral route, aerosol delivery of TB vaccines into lungs may possess special advantages, since the lung is the primary site of *Mycobacterium tuberculosis (MTB)* infection and lung macrophages are initial host cells for *MTB* (10). It has been shown that lung immunization of guinea pigs with BCG nanomicroparticles significantly reduced bacterial burden and lung pathology compared to animals immunized with standard parenteral BCG (11). However, lung delivery requires the particle size to have an aerodynamic diameter of 1–5 μm (12).

Poly (lactide-co-glycolide) (PLGA) is a copolymer that has been used in a number of FDA-approved therapeutic devices due to its biodegradability and biocompatibility (13). For example, Lupron Depot® is a commercially available drug delivery device using PLGA for the treatment of advanced prostate cancer (14,15). In addition, there have been numerous reports employing PLGA to encapsulate insulin for improved pharmacokinetics and pharmacodynamics as well as reduced dosing frequency (16–18). There exist several protocols to manufacture PLGA microparticles such as primary emulsion/spray-drying method (19), single emulsion-solvent evaporation method (20) and double emulsion-solvent evaporation method (21). An advantage with the spray-drying method lies in its scalability and reproducibility with respect to particle preparation, since each process variable associated with this technique can be well-controlled (22).

TB10.4-Ag85B is a novel TB antigen that has been previously designed in our lab by recombinant fusion of TB10.4 to the N-terminal of Ag85B (23).This molecule has

[1] Molecular Pharmaceutics, Eshelman School of Pharmacy, University of North Carolina at Chapel Hill, Chapel Hill, North Carolina 27599-7571, USA.
[2] To whom correspondence should be addressed. (e-mail: ahickey@unc.edu)

been shown to have greatly improved solubility compared to Ag85B-TB10.4 and could be purified in milligram quantities from the soluble fraction of *E. coli* culture (23). TB10.4 is a protein belonging to the 6-kDa early secretory antigenic target (ESAT-6) family comprising culture filtered protein 10 (CFP-10), ESAT-6, TB10.3 and TB10.4 *etc.* (24,25). TB10.4 was strongly recognized by BCG-vaccinated donors and was even more strongly recognized in TB patients compared to ESAT-6 (26). Ag85B is among the most potent antigen species yet identified, inducing both humoral and cell-mediated immune responses in *MTB*-infected patients (27,28). It has been shown that recombinant Ag85B encapsulated in PLGA microspheres could induce a significant amount of interleukin-2 (IL-2) production in an *in vitro* antigen presentation assay (19).

Both CD4 and CD8 T cell responses are important immunological responses for the control of *MTB* infection, among which major histocompatibility complex class II (MHC II)-dependent activation of CD4 T cells was believed to play the key role (10,29). MHC II epitopes are first processed inside the endosomes of antigen-presenting cells (APCs) and presented in the context of MHC II complex to CD4 T cells *via* cell-cell interaction and signal transduction (30). This process was mimicked by an *in vitro* antigen presentation assay developed by Boom's group, which employed THP-1 cell as an APC and DB-1T hybridoma as the CD4 T cell specific for an MHC II epitope in Ag85B ($Ag85B_{97\text{-}112}$) (31). DB-1 activation leads to IL-2 secretion, which can be easily quantified by ELISA. This assay has been successfully employed to evaluate Ag85B-specific immune response *in vitro* (19).

In the present study, the novel fusion TB antigen TB10.4-Ag85B was encapsulated into PLGA microparticles by primary emulsion/spray-drying method. The spray-drying condition was systemically optimized with respect to both particle size and yield. The resulting particles were extensively characterized by several physical methods. Comparisons were made between different formulations with respect to inducing Ag85B-specific immune response *in vitro*. The kinetics of antigen presentation were also evaluated for PLGA-MDP-TB10.4-Ag85B.

MATERIALS AND METHODS

Preparation of Recombinant Antigens

Recombinant antigens Ag85B, TB10.4 and TB10.4-Ag85B were expressed in *E. coli* and purified by a combination of nickel-affinity and size-exclusion chromatography as described previously (23). Endotoxin in the protein preparations was removed by Detoxi-Gel™ Endotoxin removing Gel (Pierce, Rockford, IL). The homogeneity of purified antigens was determined by SDS-PAGE under reducing conditions.

Microparticle Preparation

Poly (lactide-co-glycolide) (PLGA, lactic/glycolic ratio 75:25, MW 84.7 kDa, intrinsic viscosity 0.68 dL/g in $CHCl_3$) was purchased from Durect (Lactel® Absorbable Polymers, Pelham, AL, USA). Muramyl dipeptide (MDP) was purchased from Sigma (St. Louis, MO, USA). Dichloromethane (DCM) was purchased from Burdick & Jackson (HPLC grade, Muskegon, MI, USA). To optimize spray-drying condition, PLGA (700 mg) was dissolved in 200 ml DCM (0.35%, w/v). MDP (adjuvant, 3.5 mg) and bovine serum albumin (BSA, 1 mg) were dissolved in 2.4 ml phosphate buffered saline (PBS, pH7.4). The aqueous and organic phases were probe sonicated for three 10-s periods on an ice bath immediately prior to spray-drying. The emulsion was spray-dried through a 0.7-mm diameter nozzle of a Buchi mini spray-dryer (B-191, Buchi, Flawil, Switzerland) according to the half-factorial design (Table I) constructed in the statistical software Design-Expert®. Particles were collected from the jar and cyclone wall of the spray-dryer. These particles were labeled as PLGA-MDP-BSA. To prepare particles for *in vitro* antigen presentation assay, recombinant TB antigens rather than BSA were encapsulated into PLGA microparticles with the same procedure as described above, except that they were prepared at optimized spray-drying condition. These formulations include PLGA, PLGA-MDP, PLGA-MDP-TB10.4, PLGA-MDP-Ag85B, PLGA-MDP-TB10.4+Ag85B and PLGA-MDP-TB10.4-Ag85B.

Characterization of PLGA Microparticles

Projected area diameter and particle morphology were examined by a scanning electron microscope (Hitachi S-4700). Stubs were coated with gold-palladium alloy using a sputter coater.

Volume median diameter (VMD, $D_{v,\,50}$) and particle size distribution expressed as span (($D_{v,\,90}$- $D_{v,\,10}$)/ VMD) were measured using a laser diffraction particle sizer (Malvern 2600, Worcestershire, UK).

Mass median aerodynamic diameter (MMAD) was measured by an eight-stage non-viable Andersen cascade impactor (Andersen, Smyrna, GA) operated at a flow rate of 60 L/min. Sodium fluorescein (1% w/w) was incorporated into PLGA-MDP-BSA microparticles during preparation. The particles were discharged from a dry powder inhaler device (Inhalator®, Boehringer Ingelheim, Germany) and sampled into the cascade impactor. Mass deposition at each stage, the sampling inlet (throat) and preseparator was calculated based on the fluorescein content assayed by UV spectrophotometry at 490 nm.

For bulk and tapped density, approximately 1 g PLGA microparticles was placed in a graduated cylinder. The mass/volume before tapping was calculated as bulk density. The tapped density was obtained following about 100 taps, which allowed the powder volume to plateau. Carr's compressibility index (CCI) was calculated as (tapped density-bulk density)/tapped density. Hausner ratio was calculated as tapped density/bulk density.

Static angle of response was measured by pouring PLGA microparticles through a glass funnel onto a flat collection surface until the angle of response did not change with the addition of powder. The angle to the horizontal surface was measured.

Thermal analyses were carried out by differential scanning calorimetry (Perkin Elmer DSC 6, Wellesley, MA). Known quantities of powders were sealed in an aluminum pan. Analyses were performed at a ramp rate of 10°C/min.

Zeta potential was measured in a Malvern Zetasizer (NanoZS, Malvern Instruments Inc., Worcestershire, UK) for

Table I. Half Factorial Design (2^{5-1}) for the Optimization of Spray-Drying Parameters

Run	Factor 1	Factor 2	Factor 3	Factor 4	Factor 5	Res1	Res2	Res3	Res4
	Atomization	Spray Flow	Inlet Temp	Aspirator	Pump	VMD	Yield	Mode	Span
	Bar	L/hr	°C	%	ml/min	μm	%		
1	4	700	75	100	8	2.79	27.86	1	0.76
2	3	550	65	75	6	3.87	42.32	2	0.92
3	2	400	75	100	8	6.40	66.71	3	1.80
4	2	400	55	50	8	9.58	46.57	2	1.56
5	4	700	55	50	8	4.21	5.86	2	0.95
6	2	700	75	100	4	2.98	22.14	2	1.10
7	3	550	65	75	6	3.77	39.66	2	0.88
8	4	700	75	50	4	3.26	6.43	2	0.78
9	2	700	55	50	4	5.05	1.14	2	1.03
10	2	400	75	50	4	5.74	47.00	2	1.25
11	4	400	55	50	4	7.74	46.71	1	1.33
12	4	400	75	50	8	6.28	45.14	1	1.37
13	4	400	55	100	8	8.27	69.57	2	1.54
14	3	550	65	75	6	3.75	39.32	2	0.91
15	2	700	55	100	8	3.32	24.29	2	0.98
16	2	700	75	50	8	4.27	2.86	2	0.89
17	4	400	75	100	4	5.43	49.86	2	1.36
18	2	400	55	100	4	7.19	64.57	3	1.62
19	3	550	65	75	6	3.80	40.57	2	0.90
20	4	700	55	100	4	3.06	18.71	1	0.65

Labeled in red are four experimental runs to check reproducibility

0.2 mg/ml PLGA microparticles suspended in PBS thermostated at 37°C.

Surface free energy of PLGA particles was studied by inverse gas chromatography with a Hewlett-Packard 5890 Series II GC as described previously (32). A series of alkanes (C6-C10) were used as probes.

SDS-PGAE Analysis of Antigen Integrity

To study the effect of spray-drying on antigen integrity, 5 mg PLGA microparticles encapsulating different antigens were weighed after two-month storage. 300 μL SDS sampling buffer with DTT as the reducing agent was added into microparticles and extracted for 30 min at room temperature. The mixture was then boiled for 5 min at 95°C to denature the protein followed by centrifugation at 12, 000 g for 10 min. 5 μg soluble antigens were also boiled for 5 min at 95°C after mixing with SDS sampling buffer containing DTT. 20μL samples from each preparation were loaded into a 12% SDS-PAGE gel (Biorad, Hercules, CA). Proteins were visualized by Coomassie Blue staining.

Release From PLGA Microparticles

Microparticles (90 mg) of PLGA-MDP-TB10.4-Ag85B were put into 5 ml PBS (0.1% Tween 80) solution, and shaken in 37°C water bath. A volume of 0.6 ml suspension was removed at selected intervals and centrifuged for 10 min at 8, 000 g. 0.5 ml of supernatant was removed to measure the concentration of TB10.4-Ag85B and MDP. The rest of the sample and 0.5 ml fresh medium were added back into the dissolution vial. Bicinchoninic acid assay was used to determine antigen concentration, and MDP was quantified by HPLC. HPLC conditions for MDP were C18 reversed phase column (4.6×25 mm), mobile phase: 95% phosphate buffer (25 mM, pH 3.0) and 5% methanol at a flow rate of 1 ml/min and UV wavelength of 200 nm.

Cells and Media

THP-1 cells (American Type Culture Collection) were maintained in RPMI 1640 (Invitrogen Corp., Grand Island, NY) supplemented with 10% fetal bovine serum (FBS) (Hyclone, Logan, UT), 50 μM 2-mercaptoethanol, 1 mM sodium pyruvate, nonessential amino acids, 1% antibiotics/antimycotics (Invitrogen Corp., Grand Island, NY). The CD4 T-hybridoma DB1 cells (kindly provided by Dr. W. Henry Boom, Case Western Reserve University) were derived from transgenic mice with human MHC genes for HLA-DR1. They are restricted to human HLA alleles and respond to human MHC molecules presenting $Ag85B_{97–112}$ epitope. DB-1 cells were maintained in DMEM (Invitrogen Corp., Grand Island, NY) supplemented as indicated above (complete DMEM). Infection medium was DMEM supplemented with 10% non-heat-inactivated FBS with antibiotics/antimycotics.

In Vitro Antigen Presentation Assay

The anitigenicity of recombinant TB antigens was evaluated by a modified CD4 T cell hybridoma recognition assay. THP-1 cells were incubated in 96-well flat-bottom plates (10^5 cells/well) with 20 ng/ml of phorbol myristate acetate (PMA, Sigma, St Louis, MO) in infection medium for 24 h to promote adherence. Cells were washed once with PBS and incubated with 5 ng/ml of recombinant human IFN-γ(Endogen, Woburn, MA) for 24 h. The cells were washed

twice with PBS prior to antigen exposure. Antigen solutions were added at 28 ng/well into THP-1 cells. Antigens encapsulated in PLGA microparticles were added at the same concentration. DB1 T-hybridoma cells (10^5 cells/well) were added 12 h later after antigen exposure. The cells were co-incubated at 37°C for 24 h, and supernatants were harvested to measure the amount of IL-2 secreted by DB-1 by IL-2 ELISA (Biosource, Camarillo, CA).

Six-Day Antigen Presentation Assay

THP-1 cells (10^5 cells/well) were first stimulated with PMA and IFN-γ as described above and then pulsed either with 5μg soluble TB10.4-Ag85B or 28 ng TB10.4-Ag85B encapsulated in PLGA-MDP-TB10.4-Ag85B microparticles followed by further incubation for 6 h. The cells were then washed extensively with PBS to remove the antigen solution or microparticles. DB-1 (10^5 cells/well) were added at each time point (from day 1 to 6). After 24 h co-incubation, the supernatant was harvested for IL-2 ELISA assay.

Cell Viability Assay

THP-1 cells (10^5 cells/well) were plated in 96-well plates and stimulated with PMA and IFN-γ as described above. THP-1 cells were exposed to microparticles at various concentrations for 24 h. 3-(4,5-Dimethylthiazol-2-yl)-2,5-diphenyltetrazolium bromide (MTT) at 0.5 mg/ml was added into each well and incubated for 4 h. The supernatant was then removed, and 200μl of DMSO was added into the well to dissolve formazan crystals. The formazan was quantified by measuring the absorbance at the wavelength of 570 nm. Cell viability was normalized by calculating the percentage of formazan formed by cells treated with microparticles to that formed after incubation of cells in a particle-free medium.

Statistical Analysis

Multivariate statistical analysis was performed in Design-Expert® software to optimize spray-drying conditions. ANOVA was used for other analyses.

RESULTS

Half-Factorial Design for Optimization of Spray-Drying Parameters

Spray-drying was employed to produce poly (lactide-co-glycolide) (PLGA) microparticles. Variables playing pivotal roles in the spray-drying process include atomization pressure, spray flow, aspirator flow, inlet temperature and pump feeding rate. In order to dissect out the contribution of each variable and their interactions with respect to achieving favorable particle properties, a half-factorial design (2^{5-1}) was constructed in Design-Expert® as shown in Table I (16 design points plus 4 midpoints to check reproducibility), where five process variables and four response variables were listed with corresponding set and measured values. Among the four response variables, volume median diameter (VMD) and the yield were used to optimize the spray-drying parameters simultaneously. The optimization criteria were as follows: a) a VMD around 3μm (greater macrophage uptake), b) a yield greater than 15% (cost), c) a single mode of size distribution and a span less than 1 (uniformity) and d) mass median aerodynamic diameter (MMAD) between 1 and 5μm (aerosol delivery to the lung). Among these, MMAD was not an independent variable since it was determined by VMD, particle density, aggregation states and dispersion.

Analysis of Spray-Drying Parameters with Respect to Size and Yield Respectively

Process variables were first analyzed with respect to size (VMD), since this is the most important factor determining particle aerosolization and macrophage uptake. The half-normal plot in Fig. 1a suggests that spray flow (B), inlet temperature (C), aspirator flow (D) and the interaction between spray flow and inlet temperature (BC) are main contributors in determining particle size. B and C contribute almost 75% of the overall effect, while together with D and BC, they contribute almost 85% of the overall effect based on statistical analysis (not shown). Pump feeding rate and atomization pressure showed minimal effect on particle size in the test range. According to above analysis, spray flow and inlet temperature deserve most attention with respect to target particle size. As shown in Fig. 1b, VMD decreased when spray flow and inlet temperature increased. In addition, VMD was more sensitive to spray flow.

Process variables were next analyzed with respect to the yield. Fig. 1c clearly suggests that only spray flow (B) and aspirator flow (D) have statistically significant contributions. Spray flow accounts for 80% of the overall effect, and aspirator flow accounts for 15% of the overall effect according to statistical analysis (not shown). However, it should be noticed that the effect of spray flow is negative, indicating that particle yield decreased with the increase of spray flow. None of the other variables or interactions was statistically significant. Therefore, attention should be drawn to these two variables to achieve greater yield.

Simultaneous Optimization of Spray-Drying Parameters

Multivariate statistical analysis was employed to optimize spray-drying parameters to achieve target particle properties proposed above. A desirability function was used to make an overall assessment of the desirability of the combined response variables, particle size and yield. In the desirability plot as shown in Fig. 1d, only one parameter combination (marked by the red dot) leads to a desirability of 1, while all other combinations give rise to 0. The optimized spray-drying conditions are as follows: atomization pressure (3 bars), spray flow (700 L/hr), pump feeding rate (4 ml/min), aspirator flow (100%) and inlet temperature (55°C). Although the mode and span listed in Table I were not used for optimization, particles prepared by the optimized condition showed a unimodal and narrow size distribution, which meet the proposed criteria for optimization.

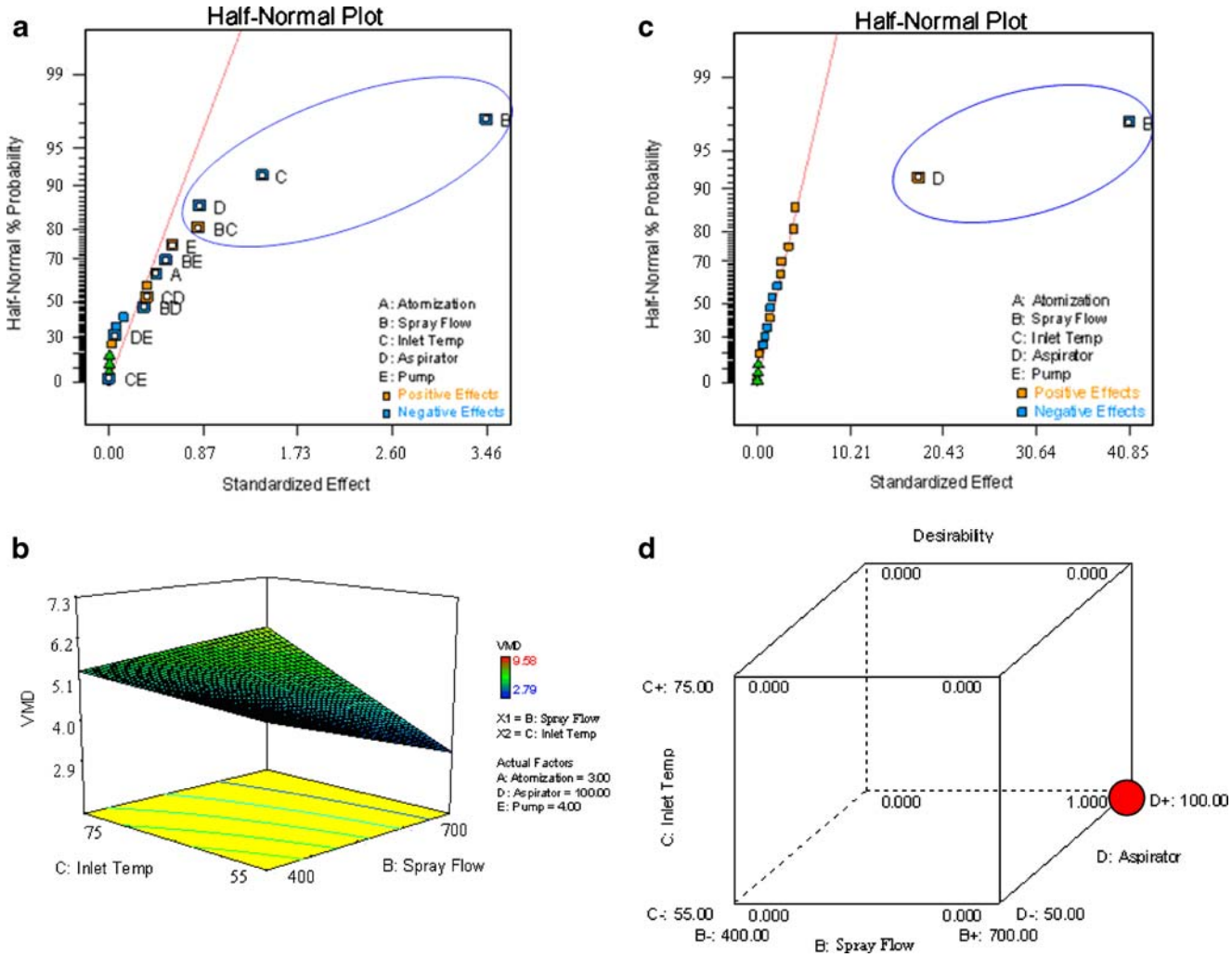

Fig. 1. Optimization of spray-drying parameters. **a**, half-normal plot with respect to particle size (VMD); **b**, response surface plot of particle size (VMD) as a function of spray flow and inlet temperature; **c**, half-normal plot with respect to particle yield; **d**, desirability plot with respect to the simultaneous optimization of both particle size (VMD) and yield.

Morphology Analysis of Spray-Dried PLGA Microparticles

First, 6 batches of particles with a VMD around 3 μm and 1 batch with the largest VMD from the optimization experiments were selected and imaged by SEM (Fig. 2a). The projected area diameter revealed by SEM images was always smaller than VMD obtained from the laser diffraction experiment (Fig. 2a). Spray-dried PLGA particles showed a wrinkled and irregular surface morphology for all batches except the one with a VMD of 9.58 μm. Particles prepared for antigen presentation assay were also imaged by SEM as shown in Fig. 2b; these particle preparations all had very similar surface morphology, although different proteins were encapsulated, indicating a high reproducibility of particle preparation at the optimized spray-drying conditions.

Particle Size Analysis of PLGA Microparticles

Particle sizes for six formulations were listed in Table II. All formulations have a VMD of approximately 3.0 μm, $D_{v,\,10}$ of 2.2 μm and $D_{v,\,90}$ of 4.4 μm. Again, these data suggested a high reproducibility of particle preparation at the optimized conditions. These particles were then analyzed with respect to the aerodynamic diameter. Fig. 3a suggests that 80% of the total mass was deposited inside the impactor, yet very little deposition was observed below 1.1 μm. Fine particle fraction (FPF) of the emitted dose was 61.5±6.4%, and FPF of the total dose was 37.0±5.5%. It should be noted that particle size distribution deviated from the ideal log-normal distribution with a MMAD of 3.3±0.2 μm and GSD of 2.7±0.1 (Fig. 3b).

Physical Characterization of PLGA Microparticles

The flow characteristics of PLGA microparticles were first evaluated. The bulk density of these powders is 0.083 g/ml. The tap density is 0.11 g/ml. Calculated Carr's compressibility index (CCI) is 24.5%, and Hausner ratio is 1.32. The static angle of response for these powders is 37±2°. All these data suggest that PLGA microparticles have intermediate flow characteristics. Thermal analysis in Fig. 4a suggests that all formulations have very similar glass transition temperature (Tg) of approximately 44°C. Detailed thermodynamic parameters were calculated and listed in Table III, which again showed almost equivalent thermal behavior for all formulations. The dispersive surface

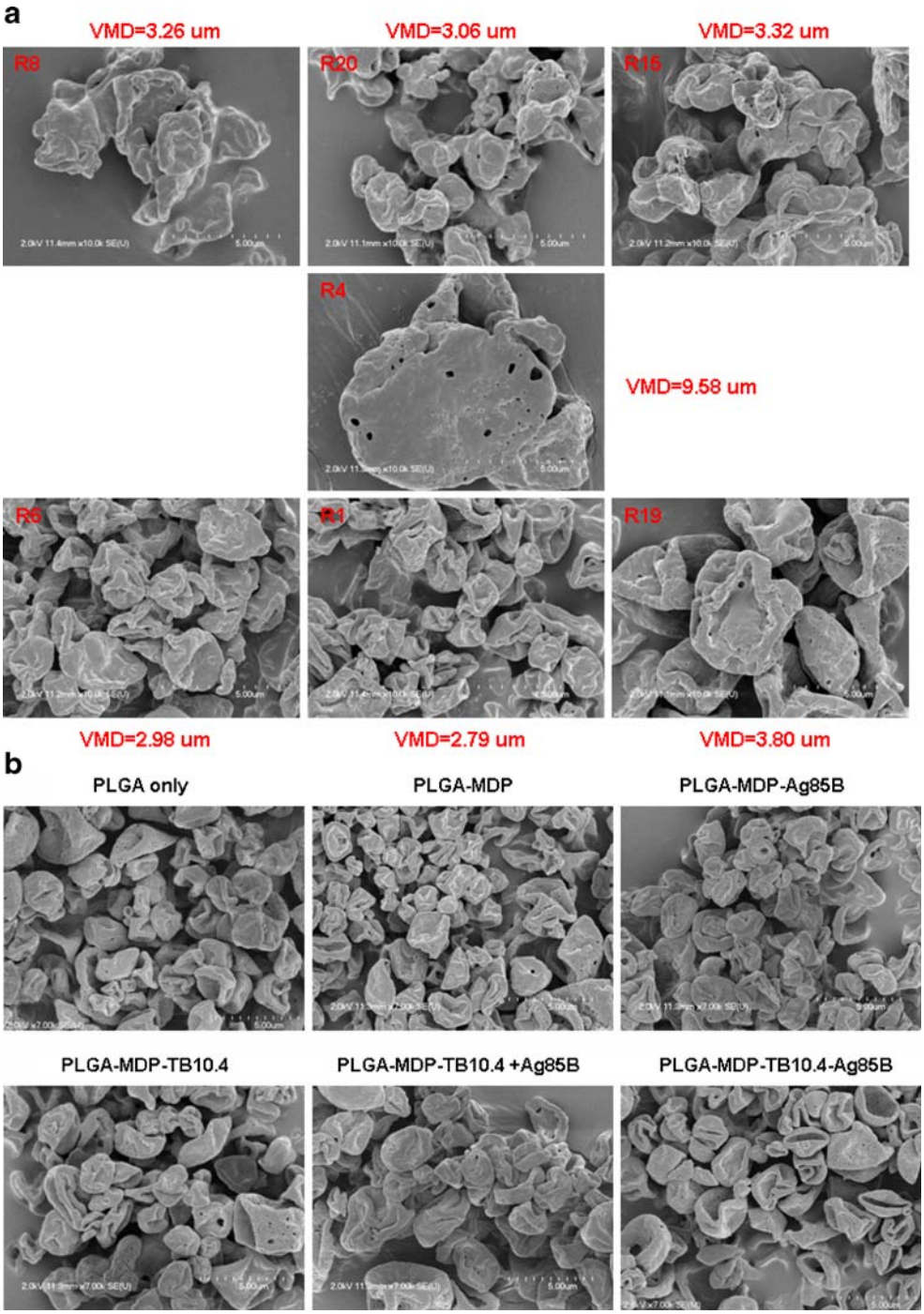

Fig. 2. Morphology analysis of spray-dried PLGA microparticles. **a**, SEM images of seven batches of microparticles prepared according to the half-factorial design. Experimental run numbers labeled in fig. **a** correspond to the run number in Table I; **b**, SEM images of PLGA microparticles prepared for antigen presentation assay under optimized spray-drying conditions.

free energy of PLGA microparticles at 25°C is 31.65 mJ/m^2 based on IGC analysis is shown in Fig. 4b. These particles were all negatively charged with a zeta potential of approximately −25 mV for all formulations (Table II, last column). SDS-PAGE was performed to investigate whether spray-drying or PLGA encapsulation compromised antigen integrity. As shown in Fig. 4c, antigens prior to and post encapsulation migrated to the same position. No degradation or truncated fragments were visible on the gel.

Release Profiles of PLGA Microparticles

The release of TB10.4-Ag85B and MDP from PLGA microparticles was characterized in a 10-day period. As shown in Fig. 5, MDP exhibited almost complete burst release during the first half hour and no release from subsequent sampling period. In contrast, TB10.4-Ag85B showed an initial burst release of 58% in the first half hour. Subsequent release exhibited a sustained manner with another 25% released during the first six-

Table II. Particle Size and Surface Charge Characterization of Spray-Dried PLGA Microparticles

Formulation	$D_{v,10}$ (μm)	$D_{v,50}$ (μm)	$D_{v,90}$ (μm)	Zeta Potential (mV)
PLGA	2.36±0.06	3.06±0.06	4.34±0.34	−26.8±5.2
PLGA-MDP	2.21±0.07	2.97±0.08	4.53±0.26	−25.7±4.7
PLGA-MDP-Ag85B	2.16±0.08	3.10±0.10	4.26±0.32	−25.2±4.9
PLGA-MDP-TB10.4	2.43±0.05	3.02±0.09	4.45±0.28	−26.1±5.0
PLGA-MDP-TB10.4+Ag85B	2.27±0.08	2.95±0.12	4.58±0.41	−24.4±5.1
PLGA-MDP-TB10.4-Ag85B	2.12±0.06	3.08±0.07	4.31±0.35	−24.6±3.9

day period. Very similar release profiles were observed for other formulations (data not shown), suggesting highly reproducible PLGA microparticle preparations.

PLGA Microparticles Encapsulating Antigens Induced Ag85B-Specific Immune Response *In Vitro*

THP-1 cells were employed as antigen presenting cells in this assay. The viability of THP-1 cells was first studied under a series of PLGA particle concentrations (Fig. 6a). Two-way ANOVA analysis suggests that there is no significant difference among formulations ($P>0.05$), among concentrations ($P>0.05$), and no interactions between two factors ($P>0.05$). Therefore, the viability of THP-1 cells was not compromised by microparticle treatment compared to medium control in the test concentration range. A dose of 20 μg/well PLGA microparticles was selected for the following studies. The concentration of encapsulated antigens was 28 ng/well at such dose.

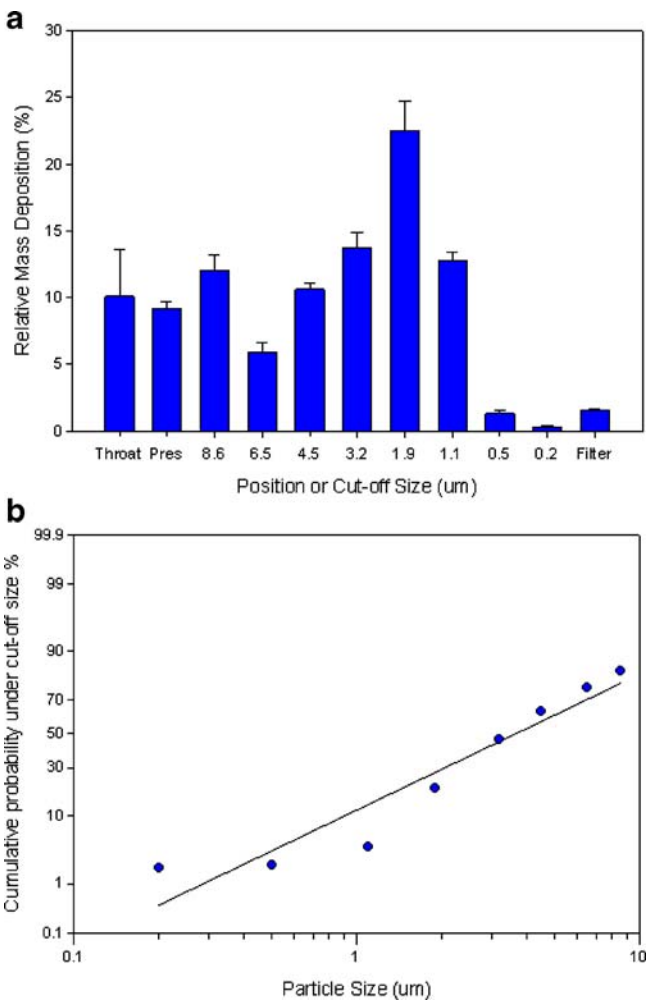

Fig. 3. Aerodynamic particle size analysis of spray-dried PLGA microparticles prepared under optimized conditions. **a**, relative mass deposition measured by Andersen cascade impactor ($n=3$, mean ± SD); **b**, log-probability plot of the mass distribution shown in **a**.

Ag85B specific *in vitro* immune response was first compared at day 1 as shown in Fig. 6b. Not surprisingly, neither control PLGA nor PLGA-MDP-TB10.4 induced IL-2 secretion due to the absence of Ag85B specific epitope. Particles encapsulating Ag85B induced the strongest IL-2 secretion. Compared to Ag85B, there was 24.7% decrease in IL-2 secretion induced by particles encapsulating both Ag85B and TB10.4 ($p<0.05$). IL-2 secretion elicited by particles encapsulating the fusion antigen TB10.4-Ag85B was further decreased by 54.8% compared to the blend of Ag85B and TB10.4 ($p<0.05$). However, it should be noticed that antigen solutions at the same concentration failed to induce IL-2 secretion at all.

Prolonged epitope presentation may be an advantageous property for a vaccine. The ability of PLGA-MDP-TB10.4-Ag85B to present epitope over time was studied (Fig. 6c). In this experiment, TB10.4-Ag85B solution was used at a concentration of 178-fold higher (5 μg/well), since it failed to induce IL-2 secretion at the same concentration as in the particle formulation (28 ng/well, Fig. 6b). Although a much higher concentration was used, IL-2 elicited by TB10.4-Ag85B solution was continuously lower than that induced by the particle formulation. For TB10.4-Ag85B solution, IL-2 secretion peaked at day 2 yet decreased rapidly afterwards, and only 20% of the peak IL-2 concentration was observed at day 6. In contrast, PLGA particles encapsulating TB10.4-Ag85B induced a prolonged IL-2 secretion. IL-2 concentration was fairly stable in the first 4 days and declined afterwards. However, 74% of the peak IL-2 was still observed at day 6.

DISCUSSION

The half-factorial design (2^{5-1}) reduced the number of spray-drying experiments from 2^5 to 2^4. An advantage of this particular design lies in that it is a resolution V design, which means that both main effects and two-factor interactions are not confounded with each other. Particle size is the most important particle property which affects both lung deposition and alveolar macrophage uptake (33–36). Hirota *et al.* reported that the most efficient delivery of rifampicin-loaded PLGA microspheres into alveolar macrophage was achieved by the phagocytosis of 3 μm particles (33). Therefore, a volume median diameter (VMD) of 3 μm was

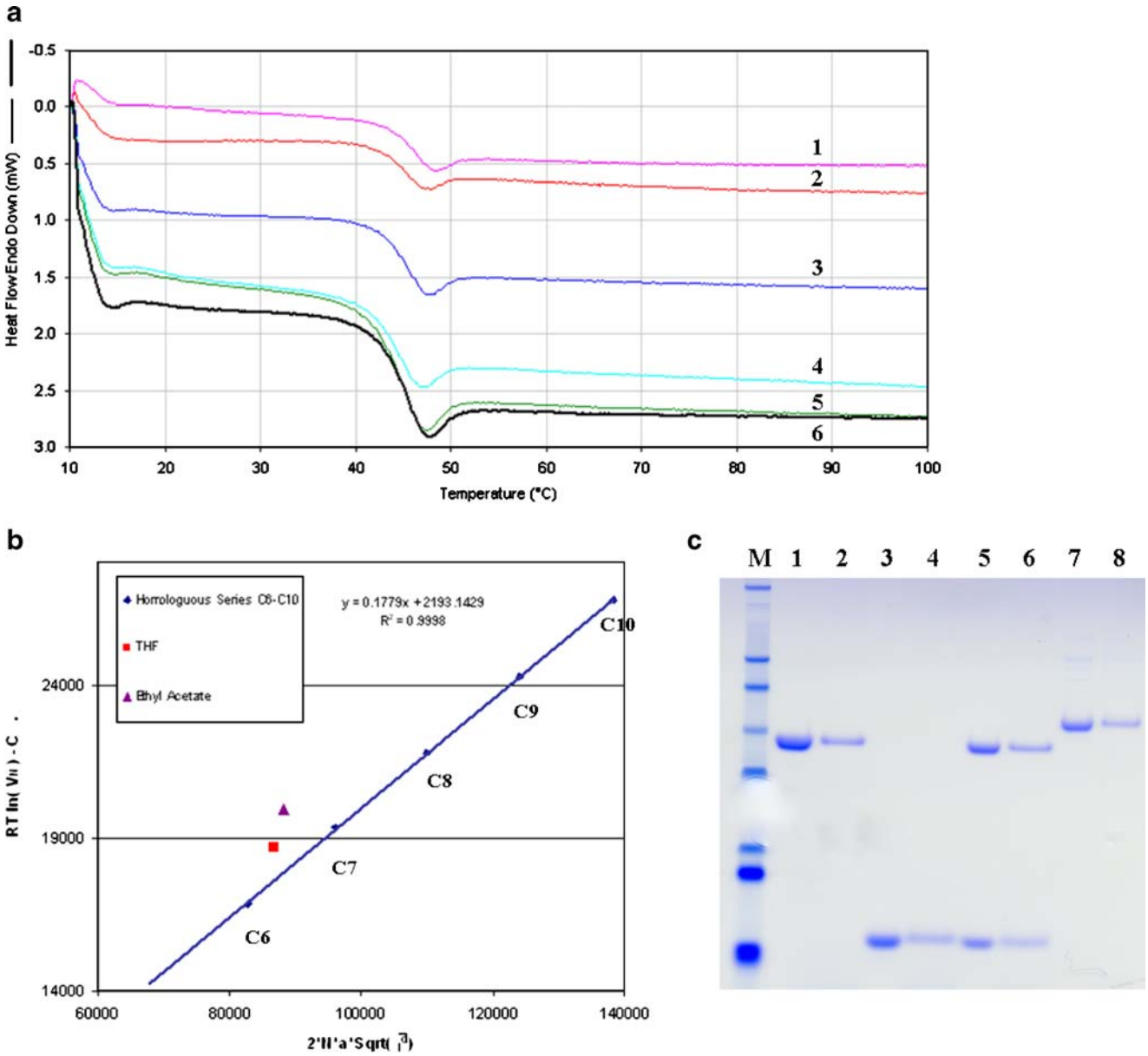

Fig. 4. Physical characterization of spray-dried PLGA microparticles. **a**, thermal characterization by differential scanning calorimetry (n=3, mean ± SD, 1: PLGA, 2: PLGA-MDP-TB10.4-Ag85B, 3: PLGA-MDP-Ag85B, 4: PLGA-MDP-TB10.4+Ag85B, 5: PLGA-MDP-TB10.4, 6: PLGA-MDP); **b**, surface energy analysis by inverse gas chromatography; **c**, SDS-PAGE analysis of antigen integrity after spray-drying (lane 1: Ag85B (s: solution), 2: Ag85B (p: powder), 3: TB10.4 (s), 4: TB10.4 (p), 5: TB10.4+Ag85B (s), 6: TB10.4+Ag85B (p), 7: TB10.4-Ag85B (s), 8: TB10.4-Ag85B (p)). Difference in band intensity was due to different loading.

selected as the optimization target. Statistical analysis showed that spray flow and inlet temperature were main contributors in determining particle size, by reducing droplet size and facilitating evaporation rate respectively. Unexpectedly, atomization pressure showed minimal effect on particle size, but, however, did affect the maximal spray flow achieved at given pressure. With respect to particle yield, only spray flow and aspirator flow were significant contributors, yet they

Table III. Thermal Characterization of Spray-Dried PLGA Microparticles (n=3, Mean±SD)

Formulation	ΔCp (J/g*°C)	Tg onset (°C)	Tg end (°C)	Tg (°C)
PLGA	0.478±0.014	43.6±0.2	46.7±0.1	44.9±0.1
PLGA-MDP	0.476±0.008	42.2±0.1	45.9±0.1	43.9±0.1
PLGA-MDP-Ag85B	0.495±0.010	42.6±0.1	45.8±0.2	44.0±0.2
PLGA-MDP-TB10.4	0.451±0.018	41.9±0.2	45.5±0.1	43.5±0.1
PLGA-MDP-TB10.4+Ag85B	0.456±0.011	41.6±0.2	45.1±0.0	43.1±0.0
PLGA-MDP-TB10.4-Ag85B	0.473±0.013	42.9±0.3	45.6±0.2	43.8±0.3

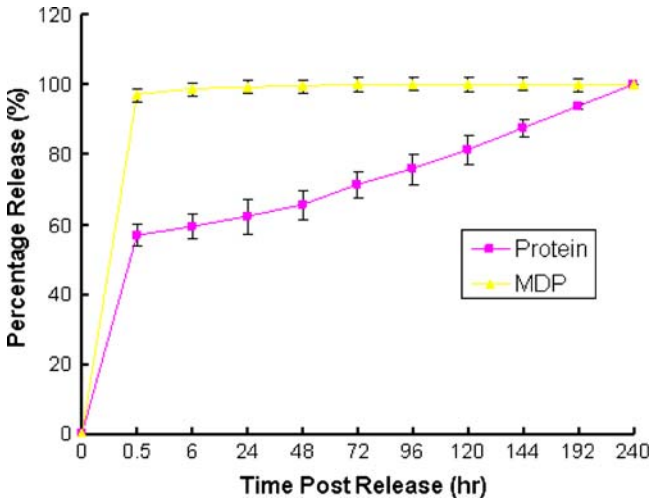

Fig. 5. Release of TB10.4-Ag85B and MDP from PLGA-MDP-TB10.4-Ag85B microparticles (n=3, mean ± SD).

exerted effects in the opposite direction. Smaller droplet was created by higher spray flow, thus collected less efficiently by the centrifugal force. Higher aspirator flow created greater centrifugal force, thus increasing the collection efficiency. Interestingly, no interaction between these two factors was observed. In addition to particle size and yield, the risk of thermal denaturatoin of antigens during spray-drying should be considered. As reported previously in our lab, the melting temperature for Ag85B and TB10.4-Ag85B was 73.7°C and 75.1°C, respectively (23). Therefore, the inlet temperature was kept as low as 55°C to avoid potential antigen denaturation. Spray flow was maintained at high level (700 L/h) for acceptable particle sizes. Maximal aspirator flow was used to compensate the low yield caused by high spray flow.

PLGA particles were frequently spheres prepared by the double emulsion-solvent evaporation method (21,37). In contrast, particles prepared by primary emulsion/spray-drying method showed irregular surface morphology, in agreement with previous report (19,38). Such morphology may explain why particles with a VMD of 3 μm had a mass median aerodynamic diameter (MMAD) of 3.3 μm. MMAD is correlated with VMD by multiplying the square root of particle density (38). Theoretically, the low density nature of PLGA particles should result in significantly smaller MMAD than VMD. However, the irregular surface morphology of PLGA particles may greatly increase the contact surface area of nearby particles, which again increased particle aggregation. These aggregates may be partly deaggregated after being discharged from the dry powder inhaler, yet a complete dispersion of particles was not achieved. This may also explain why few particles were deposited on stages with cutoff diameters less than 1.1 μm (Fig. 3a), resulting in a distribution significantly deviating from ideal log-normal distribution (Fig. 3b). Therefore, although PLGA particles prepared under optimized conditions showed narrow primary size distributions, they underwent incomplete deaggregation and existed as heterologous aggregates when delivered as aerosols. However, the MMAD and fine particle fraction of the aerosols were still acceptable, and no excipients, such as lactose, were blended with PLGA particles.

Thermal analyses of PLGA particles revealed a glass transition temperature (Tg) of approximately 44°C. This temperature had important implications for particle storage. Polymers exist in rubbery state above Tg and have increased mobility compared to the glassy state (39). Polymer annealing would likely to occur above this temperature, which may affect

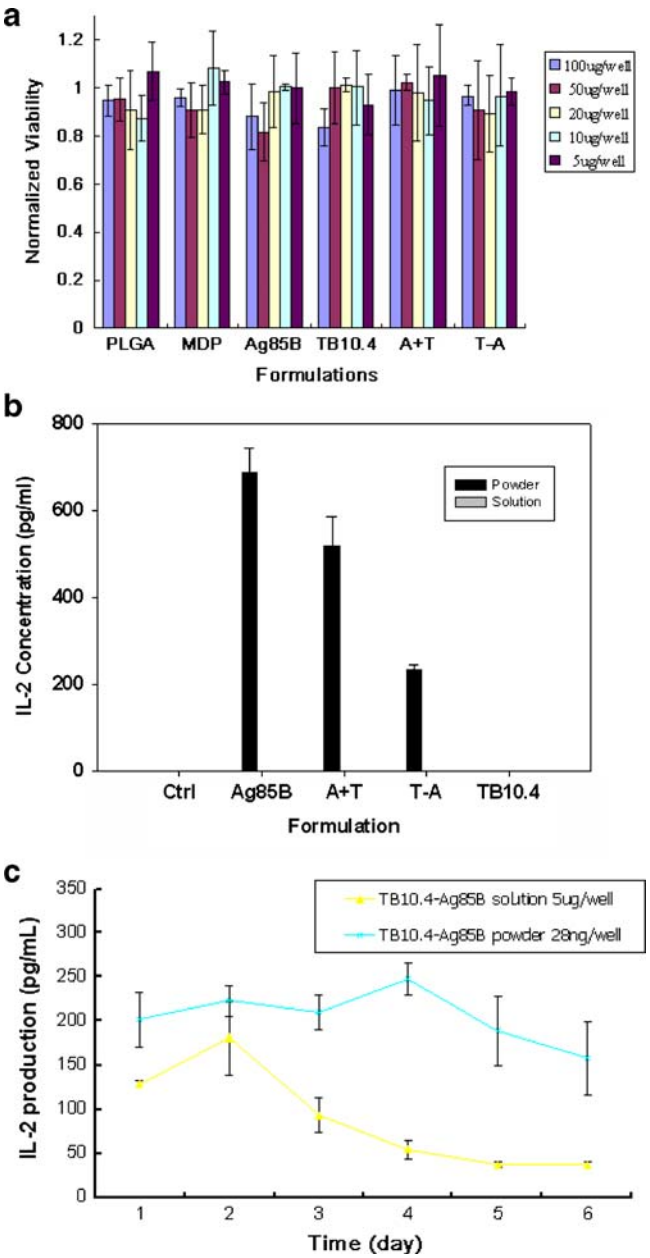

Fig. 6. *In vitro* immune response to different formulations as measured by IL-2 ELISA. **a**, viability study of THP-1 cells treated by different formulations (MDP: PLGA-MDP, Ag85B: PLGA-MDP-Ag85B, TB10.4: PLGA-MDP-TB10.4, A+T: PLGA-MDP-Ag85B+TB10.4, T-A: PLGA-MDP-TB10.4-Ag85B, n=3, mean ± SD, for all formulations); **b**, *in vitro* immune response elicited by different formulations at day one (powder: antigens encapsulated in PLGA microparticles, antigen dose = 28 ng/well; solution: antigen solutions, dose=28 ng/well, n=3, mean ± SD, Ctrl: PLGA microparticles w/o antigen); **c**, kinetic study of epitope presentation by THP-1 cell derived macrophages pulsed with PLGA-MDP-TB10.4-Ag85B (n=3, mean ± SD).

particle morphology, microstructure and ultimately the release kinetics of encapsulated antigens (40). In order to minimize polymer annealing, PLGA particles should be stored below the Tg. In addition, moisture contact should be avoided, since water serves as a plasticizer to lower the Tg (41). Therefore, PLGA particles are recommended to store with desiccant at either room temperature or in the refrigerator.

Emulsifiers were not used to prepare the primary water-in-oil emulsion, since they might influence phagocytosis (42–44). The high initial burst of MDP and TB10.4-Ag85B from PLGA microparticles indicates that the primary emulsion was not sufficiently stable to retain the internal water phase. Therefore, it is possible that a portion of MDP and TB10.4-Ag85B are associated with microparticle surfaces after spray-drying *via* electrostatic and hydrophobic interactions (45). In addition, both MDP and TB10.4-Ag85B are water-soluble molecules immiscible with the PLGA polymer. Rather than dissolved in the matrix of PLGA, they were more likely to be dispersed in the matrix by occupying internal voids. Channels/pores may directly connect these voids to the particle surface, thus leading to a high burst release before the bulk erosion of PLGA occurs (40). All these mechanisms may explain the high initial burst. Interestingly, the sustained-release phase observed in TB10.4-Ag85B was absent for MDP. The nearly complete burst release of MDP may be partly explained by the rapid diffusion of this small molecule, which has a molecular weight two orders of magnitude below TB10.4-Ag85B. Although MDP was not shown to significantly enhance the immunogenicity of Ag85B *in vitro* (19), it might have significant effect *in vivo*, which could be compromised by the high initial burst. Efforts should be spent to optimize the release kinetics of both MDP and TB10.4-Ag85B in the future.

Antigen solutions failed to elicit IL-2 secretion at the same concentration as in the particle formulation (28 ng/well). However, IL-2 was induced by antigen solutions at much higher concentration (5 μg/well), possibly due to macropinocytosis of antigens into endosomes in a concentration-dependent manner (46). Compared to PLGA-MDP-Ag85B, which induced the highest level of IL-2 secretion, the blend of TB10.4 with Ag85B led to a reduction in IL-2 secretion, which may be explained by the competition of TB10.4 for major histocompatibility complex (MHC) molecules. The fusion of TB10.4 with Ag85B (TB10.4-Ag85B) further decreased IL-2 secretion. There are two possible explanations for this observation. First, competition may exist between TB10.4 and Ag85B for MHC molecules as mentioned above. Second, the fusion of TB10.4 with Ag85B may alter the structure of the fusion antigen and affect the processing of Ag85B epitopes inside endosomes, which may ultimately affect Ag85B specific epitope presentation. Nevertheless, a moderate decrease of Ag85B-specific immune response was not unexpected for the fusion antigen. It did not compromise the developability of TB10.4-Ag85B as the subunit vaccine, since a balanced and diversified immune response may be more favorable from a vaccine point of view (10). TB10.4-specific immune response will be investigated in the future. Six-day antigen presentation data illustrated another advantage of microparticle formulation of antigen, that is, prolonged epitope presentation favoring T cell activation. Processed epitope was first presented by MHC molecules onto the surface of antigen presenting cell (APC). This complex should be stable during the transit to the draining lymph node where T cell activation mainly occurs (47). Rapid decrease of epitope presentation by APC may compromise T cell recognition and activation.

CONCLUSION

TB10.4-Ag85B, a novel recombinant TB antigen designed previously in our lab, was developed as a PLGA particle formulation in this study. The spraying-drying condition to prepare PLGA microparticles was successfully optimized by employing the concept of quality by design (QbD). Particles with suitable sizes for pulmonary delivery were obtained and characterized extensively with respect to their physical properties. PLGA-MDP-TB10.4-Ag85B induced much stronger Ag85B-specific immune response *in vitro* at much lower concentration compared to antigen solutions. This formulation also provided prolonged epitope presentation up to 6 days. Taken together, these data suggest that dry powder delivery of recombinant TB10.4-Ag85B in a microparticle formulation has potential as a vaccine strategy for preventing *MTB* infection or as a promising boosting vaccine.

ACKNOWLEDGEMENT

The authors greatly appreciate the technical assistance offered by Amar Kumbhar for SEM imaging. The authors are also thankful to Dr. Jian Liu for offering the FPLC to purify recombinant TB antigens. DB-1 hybridoma cells were kindly supplied by Dr. Henry Boom of Case Western Reserve University.

REFERENCES

1. Dunlap NE, Briles DE. Immunology of tuberculosis. Med Clin North Am. 1993;77:1235–51.
2. Flynn JL, Chan J. Immunology of tuberculosis. Annu Rev Immunol. 2001;19:93–129.
3. Brimnes N. BCG vaccination and WHO's global strategy for tuberculosis control 1948–1983. Soc Sci Med. 2008;67:863–73.
4. Colditz GA, Brewer TF, Berkey CS, Wilson ME, Burdick E, Fineberg HV, *et al.* Efficacy of BCG vaccine in the prevention of tuberculosis. Meta-analysis of the published literature. Jama. 1994;271:698–702.
5. Fine PE. Variation in protection by BCG: implications of and for heterologous immunity. Lancet. 1995;346:1339–45.
6. Sterne JA, Rodrigues LC, Guedes IN. Does the efficacy of BCG decline with time since vaccination? Int J Tuberc Lung Dis. 1998;2:200–7.
7. Rodrigues LC, Pereira SM, Cunha SS, Genser B, Ichihara MY, de Brito SC, *et al.* Effect of BCG revaccination on incidence of tuberculosis in school-aged children in Brazil: the BCG-REVAC cluster-randomised trial. Lancet. 2005;366:1290–5.
8. Mittal SK, Aggarwal V, Rastogi A, Saini N. Does B.C.G. vaccination prevent or postpone the occurrence of tuberculous meningitis? Indian J Pediatr. 1996;63:659–64.
9. Colditz GA, Berkey CS, Mosteller F, Brewer TF, Wilson ME, Burdick E, *et al.* The efficacy of bacillus Calmette-Guerin vaccination of newborns and infants in the prevention of tuberculosis: meta-analyses of the published literature. Pediatrics. 1995;96:29–35.
10. Skeiky YA, Sadoff JC. Advances in tuberculosis vaccine strategies. Nat Rev Microbiol. 2006;4:469–76.

11. Garcia-Contreras L, Wong YL, Muttil P, Padilla D, Sadoff J, Derousse J, *et al*. Immunization by a bacterial aerosol. Proc Natl Acad Sci USA. 2008;105:4656–60.
12. Gupta GA, Hickey AJ. Contemporary approaches in aerosolized drug delivery to the lung. J Control Release. 1991;17:127–47.
13. Lu JM, Wang X, Marin-Muller C, Wang H, Lin PH, Yao Q, *et al*. Current advances in research and clinical applications of PLGA-based nanotechnology. Expert Rev Mol Diagn. 2009;9:325–41.
14. Okada H. One- and three-month release injectable microspheres of the LH-RH superagonist leuprorelin acetate. Adv Drug Deliv Rev. 1997;28:43–70.
15. Okada H, Toguchi H. Biodegradable microspheres in drug delivery. Crit Rev Ther Drug Carrier Syst. 1995;12:1–99.
16. Hamishehkar H, Emami J, Najafabadi AR, Gilani K, Minaiyan M, Mahdavi H, *et al*. The effect of formulation variables on the characteristics of insulin-loaded poly(lactic-co-glycolic acid) microspheres prepared by a single phase oil in oil solvent evaporation method. Colloids Surf B Biointerfaces. 2009;74:340–9.
17. Han Y, Tian H, He P, Chen X, Jing X. Insulin nanoparticle preparation and encapsulation into poly(lactic-co-glycolic acid) microspheres by using an anhydrous system. Int J Pharm. 2009;378:159–66.
18. Kim BS, Oh JM, Hyun H, Kim KS, Lee SH, Kim YH, *et al*. Insulin-Loaded Microcapsules for *in vivo* delivery. Mol Pharm. 2009.
19. Lu D, Garcia-Contreras L, Xu D, Kurtz SL, Liu J, Braunstein M, *et al*. Poly (lactide-co-glycolide) microspheres in respirable sizes enhance an *in vitro* T cell response to recombinant Mycobacterium tuberculosis antigen 85B. Pharm Res. 2007;24:1834–43.
20. Emami J, Hamishehkar H, Najafabadi AR, Gilani K, Minaiyan M, Mahdavi H, *et al*. A novel approach to prepare insulin-loaded poly(lactic-co-glycolic acid) microcapsules and the protein stability study. J Pharm Sci. 2009;98:1712–31.
21. Kirby DJ, Rosenkrands I, Agger EM, Andersen P, Coombes AG, Perrie Y. PLGA microspheres for the delivery of a novel subunit TB vaccine. J Drug Target. 2008;16:282–93.
22. Cal K, Sollohub K. Spray drying technique. I: hardware and process parameters. J Pharm Sci. 2009.
23. Shi S, Yu L, Sun D, Liu J, Hickey AJ. Rational design of multiple TB antigens TB10.4 and TB10.4-Ag85B as subunit vaccine candidates against mycobacterium tuberculosis. Pharm Res, doi:10.1007/s11095-009-9995-y, 2009.
24. Skjot RL, Oettinger T, Rosenkrands I, Ravn P, Brock I, Jacobsen S, *et al*. Comparative evaluation of low-molecular-mass proteins from Mycobacterium tuberculosis identifies members of the ESAT-6 family as immunodominant T-cell antigens. Infect Immun. 2000;68:214–20.
25. Renshaw PS, Lightbody KL, Veverka V, Muskett FW, Kelly G, Frenkiel TA, *et al*. Structure and function of the complex formed by the tuberculosis virulence factors CFP-10 and ESAT-6. Embo J. 2005;24:2491–8.
26. Skjot RL, Brock I, Arend SM, Munk ME, Theisen M, Ottenhoff TH, *et al*. Epitope mapping of the immunodominant antigen TB10.4 and the two homologous proteins TB10.3 and TB12.9, which constitute a subfamily of the esat-6 gene family. Infect Immun. 2002;70:5446–53.
27. Daffe M. The mycobacterial antigens 85 complex — from structure to function and beyond. Trends Microbiol. 2000; 8:438–40.
28. Wiker HG, Harboe M. The antigen 85 complex: a major secretion product of Mycobacterium tuberculosis. Microbiol Rev. 1992;56:648–61.
29. Havlir DV, Wallis RS, Boom WH, Daniel TM, Chervenak K, Ellner JJ. Human immune response to Mycobacterium tuberculosis antigens. Infect Immun. 1991;59:665–70.
30. Strawbridge AB, Blum JS. Autophagy in MHC class II antigen processing. Curr Opin Immunol. 2007;19:87–92.
31. Canaday DH, Gehring A, Leonard EG, Eilertson B, Schreiber JR, Harding CV, *et al*. T-cell hybridomas from HLA-transgenic mice as tools for analysis of human antigen processing. J Immunol Methods. 2003;281:129–42.
32. Telko MJ, Hickey AJ. Critical assessment of inverse gas chromatography as means of assessing surface free energy and acid-base interaction of pharmaceutical powders. J Pharm Sci. 2007;96:2647–54.
33. Hirota K, Hasegawa T, Hinata H, Ito F, Inagawa H, Kochi C, *et al*. Optimum conditions for efficient phagocytosis of rifampicin-loaded PLGA microspheres by alveolar macrophages. J Control Release. 2007;119:69–76.
34. O'Hara P, Hickey AJ. Respirable PLGA microspheres containing rifampicin for the treatment of tuberculosis: manufacture and characterization. Pharm Res. 2000;17:955–61.
35. Shi S, Ashley ES, Alexander BD, Hickey AJ. Initial characterization of micafungin pulmonary delivery via two different nebulizers and multivariate data analysis of aerosol mass distribution profiles. AAPS PharmSciTech. 2009;10:129–37.
36. Shi S, Hickey AJ. Multivariate data analysis as a semi-quantitative tool for interpretive evaluation of comparability or equivalence of aerodynamic particle size distribution profiles. AAPS PharmSciTech, 2009.
37. Dos Santos DF, Nicolete R, de Souza PR, Bitencourt CD, Dos Santos Junior RR, Bonato VL, *et al*. Characterization and *in vitro* activities of cell-free antigens from Histoplasma capsulatum-loaded biodegradable microspheres. Eur J Pharm Sci 2009.
38. Wang C, Muttil P, Lu D, Beltran-Torres AA, Garcia-Contreras L, Hickey AJ. Screening for potential adjuvants administered by the pulmonary route for tuberculosis vaccines. Aaps J. 2009;11:139–47.
39. Nastasovic AB, Onjia AE. Determination of glass temperature of polymers by inverse gas chromatography. J Chromatogr A. 2008;1195:1–15.
40. Allison SD. Analysis of initial burst in PLGA microparticles. Expert Opin Drug Deliv. 2008;5:615–28.
41. Surana R, Randall L, Pyne A, Vemuri NM, Suryanarayanan R. Determination of glass transition temperature and *in situ* study of the plasticizing effect of water by inverse gas chromatography. Pharm Res. 2003;20:1647–54.
42. Jones BG, Dickinson PA, Gumbleton M, Kellaway IW. Lung surfactant phospholipids inhibit the uptake of respirable microspheres by the alveolar macrophage NR8383. J Pharm Pharmacol. 2002;54:1065–72.
43. Evora C, Soriano I, Rogers RA, Shakesheff KN, Hanes J, Langer R. Relating the phagocytosis of microparticles by alveolar macrophages to surface chemistry: the effect of 1, 2-dipalmitoylphosphatidylcholine. J Control Release. 1998;51:143–52.
44. Jones BG, Dickinson PA, Gumbleton M, Kellaway IW. The inhibition of phagocytosis of respirable microspheres by alveolar and peritoneal macrophages. Int J Pharm. 2002;236: 65–79.
45. Sugiyama K, Mitsuno S, Shiraishi K. Adsorption of protein on the surface of thermosensitive poly(methyl methacrylate) microspheres modified with the N-(2-hydroxypropyl)methacrylamide and 2-(methacryloyloxy)ethyl phosphorylcholine moieties. J Polymer Sci Part A Polymer Chem. 1996;35:3349–57.
46. Kerr MC, Teasdale RD. Defining macropinocytosis. Traffic. 2009;10:364–71.
47. Sant AJ, Chaves FA, Jenks SA, Richards KA, Menges P, Weaver JM, *et al*. The relationship between immunodominance, DM editing, and the kinetic stability of MHC class II:peptide complexes. Immunol Rev. 2005;207:261–78.